nature structural & molecular biology

Rates of *in situ* transcription and splicing in large human genes

Jarnail Singh & Richard A Padgett

Transcription and splicing must proceed over genomic distances of hundreds of kilobases in many human genes. However, the rates and mechanisms of these processes are poorly understood. We have used the compound 5,6-dichlorobenzimidazole 1-β-D-ribofuranoside (DRB), which reversibly blocks gene transcription *in vivo*, combined with quantitative RT-PCR to analyze the transcription and RNA processing of several long human genes. We found that the rate of RNA polymerase II transcription over long genomic distances is about 3.8 kb min^{-1} and is similar whether transcribing long introns or exon-rich regions. We also determined that co-transcriptional pre-mRNA splicing of U2-dependent introns occurs within 5–10 min of synthesis, irrespective of intron length between 1 kb and 240 kb. Similarly, U12-dependent introns were co-transcriptionally spliced within 10 min of synthesis, confirming that these introns are spliced within the nuclear compartment. These results show that the expression of large genes is unexpectedly rapid and efficient.

Transcription by RNA polymerase II (RNAPII) is a multistep process consisting of promoter binding, transcription initiation, elongation and termination. In addition, RNAPII has important roles in RNA processing events including 5′ cap formation, splicing, poly(A) tail formation, 3′ end processing and transport of the mRNA to the cytoplasm[1–6]. Much of the previous research on transcriptional regulation has focused on promoter regulation and transcription initiation. However, recent work has suggested that events subsequent to transcript initiation may be of equal or greater importance in regulating the output of genes[7–10]. Furthermore, the rate of elongation and pausing of RNAPII is emerging as a key contributory factor in the regulation of alternative splicing[7,11–13]. This in turn has generated considerable interest in the kinetics of transcriptional elongation by RNAPII.

Previous efforts to calculate the *in situ* elongation rate of RNAPII have used a range of methods including RT-PCR[14], nuclear run-on assays[15] and fluorescent *in situ* hybridization[16,17]. These studies focused on specific genes and yielded apparent elongation rate estimates ranging from 1.1 kb min^{-1} to 4.3 kb min^{-1}. More recent studies have used engineered gene constructs monitored by fluorescence imaging techniques in living cells[17,18]. Mathematical modeling was used to extract detailed kinetic information, including rates of transcriptional elongation. The calculated elongation rates derived from these studies ranged from 1.9 kb min^{-1} to 4.3 kb min^{-1}. Given the importance of post-initiation events in gene expression and the range of results produced by these methods, a simple technique capable of measuring the rates of transcription of many genes in their endogenous environments in many cell types would be a major advance.

The rate of splicing of introns *in vivo* has also been studied in a few cases. Analysis of introns of an endogenous gene[19] or of small introns in artificial gene constructs with inducible promoters[20] showed that splicing occurred on a timescale of 1–12 min. These studies examined relatively short introns. As intron length can vary from less than 100 bases to hundreds of kilobases, it would be interesting to measure splicing rates over a range of gene and intron lengths.

There is strong evidence to conclude that RNA splicing of major class or U2-dependent introns frequently occurs co-transcriptionally and is aided by the elongating RNAPII[3,21–23]. In contrast, a recent report[24] suggested that most minor class or U12-dependent spliceosome components may be localized predominantly in the cytoplasm, and therefore most if not all of the U12-dependent splicing would have to take place post-transcriptionally after the transcript is fully synthesized and transported to the cytoplasm. This study, which itself contradicted earlier results[25], prompted other reports[26,27] that demonstrated the preferential localization of U12-dependent spliceosomal RNA and protein components to the nucleus. However, in the absence of direct *in vivo* evidence on the temporal and spatial relationship of transcription and minor class intron splicing, the controversy has not been resolved[28,29].

Here we report the development of a simple assay system with which to measure the rates of RNAPII transcription and pre-mRNA splicing *in vivo* on endogenous human genes. Using the reversible inhibitor DRB, we can switch off and rapidly switch on transcription by RNAPII of many genes without any apparent detrimental effect to the cellular machinery. We report on the use of this method in conjunction with real-time quantitative RT-PCR to study the kinetics of transcription and splicing in a number of human genes in their natural chromatin environments. Our results demonstrate that RNAPII transcribes at a rate close to 3.8 kb min^{-1} over megabase distances and that the splicing of both U2-dependent and U12-dependent introns can occur rapidly and co-transcriptionally.

Department of Molecular Genetics, Lerner Research Institute, Cleveland Clinic, Cleveland, Ohio, USA. Correspondence should be addressed to R.A.P. (padgetr@ccf.org).

Received 10 February; accepted 11 August; published online 11 October 2009; doi:10.1038/nsmb.1666

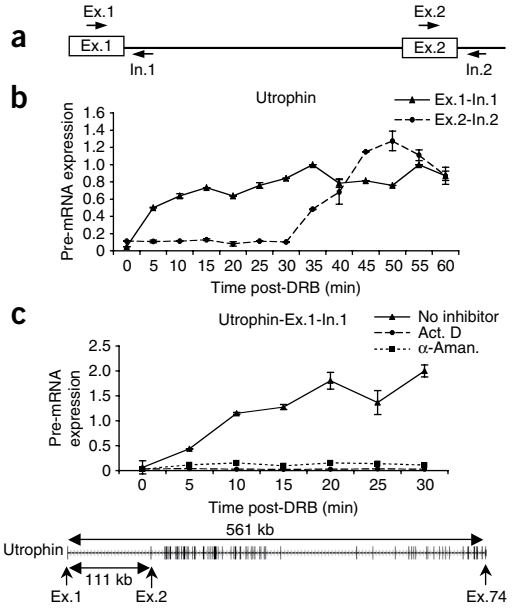

Figure 1 DRB reversibly inhibits new transcription by RNAPII. (**a**) Schematic diagram showing the primer sets used to amplify the exon (Ex.)–intron (In.) junctions of exons 1 and 2 of the Utrophin gene. (**b**) Quantitative RT-PCR was used to measure the expression levels of Utrophin pre-mRNA in the exon 1 and exon 2 regions of the gene. Cells were first treated with 100 μM DRB for 3 h, and then fresh medium was added after DRB removal. The cells were harvested at 5-min intervals for RNA isolation and quantitative RT-PCR. The expression values are plotted relative to the expression level of the 'no-treatment' control, which was set to 1 in all experiments. (**c**) Effect of actinomycin D (Act. D) and α-amanitin (α-Aman.) on transcription of the first exon-intron junction of the Utrophin gene after DRB treatment. Cells were treated with DRB for 3 h, and either actinomycin D or α-amanitin was added 30 min before the removal of DRB. Cells were released from DRB but maintained in the other drugs. Cells were harvested at 5-min intervals and quantitative RT-PCR was performed as above to measure the levels of expression of the exon 1–intron 1 region of the Utrophin gene. Shown below is the exon-intron structure of the Utrophin gene. Transcription is from left to right and the exons are represented as larger vertical bars. Error bars, s.e.m.

RESULTS

DRB inhibits the P-TEFb–dependent Ser2 phosphorylation of the C-terminal domain (CTD) of RNAPII, resulting in its failure to progress from the initiation to the elongation phase of transcription[30–33]. Notably, it does not block elongation of previously initiated transcripts already within the gene[32]. It should also be noted that, although most genes are blocked by DRB, there is a subset of promoters that do not respond to DRB[34].

We used this property of DRB to develop a method to reversibly block gene transcription in cultured human cells. We incubated the cells for various times with DRB. We then prepared total RNA from the cultures and assayed for the levels of unspliced pre-mRNA for several genes. During the time of DRB treatment, most of the unspliced pre-mRNA should be processed to mature mRNA by the splicing machinery or degraded (**Supplementary Fig. 1**). Removal of DRB should then lead to release of RNAPII from promoter-proximal regions, starting fresh rounds of transcription. These newly started primary transcripts will be detectable owing to the presence of introns.

We treated human Tet-21 cells for 3 h with DRB, taking samples at 5-min intervals after the removal of DRB. We performed quantitative RT-PCR using primers spanning exon-intron junctions to detect pre-mRNA expression (**Fig. 1a**). As a test case we focused on the 561-kb Utrophin gene. The Utrophin gene contains 74 exons and 73 introns, and its first intron is 111 kb long. Cells incubated with DRB were able to recover transcription of the exon 1 region of the Utrophin gene within minutes of DRB removal (**Fig. 1b**). In contrast, recovery of expression of the exon 2 region showed a delay until 35 min after drug release, consistent with a transcriptional lag due to the genomic distance between the first two exons. This suggests that RNAPII transcribed the 111-kb region of the Utrophin gene in roughly 30 min, at a rate of ~3.7 kb min^{-1}.

It is possible that the 3-h incubation in DRB might alter the chromatin state of the cells and thus affect the rate of transcription that we measured. To test for this, we treated Tet-21 cells for only 30 min with DRB and isolated RNA at 5-min intervals after removing the DRB. Transcription of the exon 1–intron 1 region of the 178-kb catenin, β-like 1 gene (*CTNNBL1*) recovered quickly after DRB removal, whereas the pre-mRNA signal at the intron 15–exon 16 region decayed slowly over 45 min and then recovered quickly (**Supplementary Fig. 2**). This suggests that RNAPII requires about 45 min to transcribe the 178-kb gene, giving an elongation rate of ~3.9 kb min^{-1}, which is similar to the rate seen after a 3-h DRB treatment.

Validation of the assay to study transcription elongation

To establish that the increase in pre-mRNA levels shown in **Figure 1b** for exon 1 and exon 2 of the Utrophin gene was due to new rounds of RNAPII-dependent transcription, we carried out several control experiments. Treatment with either actinomycin D or α-amanitin blocked the recovery of the pre-mRNA signal following DRB release (**Fig. 1c**). This provides clear evidence that the signal we detected in **Figure 1b** was due to transcriptional activity of RNAPII.

We interpret the time lag between the reappearance of the signals for exons 1 and 2 of the Utrophin gene to be due to elongation through the long intron that separates them. If this is true, the time lag should be sensitive to changes in the elongation rate of RNAPII. The drug camptothecin (CPT), an inhibitor of topoisomerase I, substantially reduces the rate of transcription elongation by RNAPII to about 1 kb min^{-1}, or about three to four times slower than normal[17,35–37]. Thus, if we were indeed measuring the rate of RNAPII elongation in our experiments, CPT treatment should have strongly increased the observed lag times.

To test this, we incubated DRB-treated cells in the presence of CPT for 15 min before removal of DRB and then maintained them in CPT after removal of DRB. The recovery time of gene regions downstream of the promoters of two genes were substantially lengthened, as expected (**Supplementary Fig. 3**). These results strongly support the view that these experiments measured new RNAPII transcription starting at or near the normal transcriptional start site and that the lag times observed in the expression of downstream sequences reflect the rate of elongation of RNAPII.

A concern with the above experiments is that DRB treatment might somehow alter the chromatin environment, producing an incorrect elongation rate. We therefore used an independent method to induce transcription that did not rely on DRB. Treatment of responsive cells with cytokines such as interferon-β leads to rapid induction of many genes[38]. One example is the *PKR* gene (also known as *EIF2AK2*). We treated human HT1080 cells with interferon-β and monitored the pre-mRNA levels from *PKR* at two positions that are 40 kb apart. Pre-mRNA levels rose at both sites after interferon treatment with a time difference of about 12 min, suggesting an elongation rate of ~3.3 kb min^{-1} (**Supplementary Fig. 4**). Thus, an independent method of gene induction gave an apparent RNAPII elongation rate similar to that determined using DRB.

Table 1 Rates of RNAPII elongation through various regions of different genes

Gene	Region	Length (kb)	Time to transcribe (min)	Elongation rate (kb min^{-1})
Utrophin	Ex1-Ex2	111	30	3.70
Utrophin	Ex2-Ex50	174	40	4.35
Utrophin	Ex50-Ex51	101	25	4.04
Utrophin	Ex51-Ex74	173	40	4.33
Utrophin	Ex1-Ex74	561	140	**4.01**
ITPR1	Ex1-Ex5	133	40	3.33
ITPR1	Ex5-Ex40	105	25	4.20
ITPR1	Ex1-Ex40	238	65	**3.66**
EFNA5	Ex1-Ex2	243	70	**3.47**
BCL2	Ex2-Ex3	189	50	**3.78**
OPA1	Ex1-Ex29	104	25	**4.16**
IFT80	Ex1-Ex20	142	35	**4.06**
CTNNBL1	Ex1-Ex16	178	45	**3.96**
KIFAP3	Ex1-Ex20	153	45	**3.40**
SLC9A9	Ex1-Ex16	583	160	**3.64**
Average elongation rate of all genes				3.79 ± 0.26

The elongation rates for full-length genes are shown in bold, and these values were used to compute the average and s.d. of the elongation rate for all the genes. Ex, exon.

The experimental protocols described above measure the transcriptional output of RNAPII rather than the physical presence of the polymerase in different gene regions. To demonstrate a direct relationship between the transcriptional signal and the presence of polymerase, we performed chromatin immunoprecipitation (ChIP) using antibodies against RNAPII. **Supplementary Figure 5a**,**b** shows conventional gel analysis and real-time PCR ChIP, respectively, of the promoter-proximal regions of three genes and a distal region of one. In all cases, DRB treatment for 3 h (0′ lanes) reduced the amount of RNAPII in these regions. The RNAPII signals recovered within 5 min of washing for the promoter-proximal regions and within 10 min for downstream regions.

We also examined RNAPII occupancy at gene regions far downstream of the promoter region. **Supplementary Figure 5c**,**d** show that the RNAPII ChIP signals for the inositol 1,4,5-triphosphate receptor, type 1 gene (*ITPR1*) show similar kinetics of appearance to the pre-mRNA signals (see below). These results confirm that the distribution of RNAPII reflects the RNA signals detected by RT-PCR analysis.

Elongation rates seem to be similar for most genes

Having shown that the DRB release method allows us to follow the progress of RNAPII through chromatin, we investigated the rate of transcriptional elongation in several large human genes. The selected genes are listed in **Table 1**, and the data for four of these are shown in **Figure 2**, along with their exon-intron structures.

Several results are notable. First, as shown in **Table 1**, all gene regions seemed to be transcribed with a markedly uniform rate of about 3.8 kb min^{-1}. This value is close to the maximum elongation rate (4.3 kb min^{-1}) determined by Darzacq *et al.*[17]. This suggests that, within genes in their natural chromosomal locations and chromatin states, transcription elongation can be very efficient.

A second notable result is that there seems to be a fairly consistent progression of polymerase within each gene. As can be seen for the Utrophin gene shown in **Figure 2a**, there is relatively little dispersion of the signals as transcription proceeds through hundreds of kilobases of DNA. Even at the end of the 561-kb gene (exon 74), there is a sharp rise in the signal between 10-min time points. This suggests that transcription elongation is highly uniform over individual genes in a cell population.

Third, the data suggest that there is little or no difference in elongation rate through gene regions that contain few or no exons (and thus long introns) compared to regions that contain multiple exons and short introns. Two of the genes shown in **Figure 2**, Utrophin and *ITPR1*, have structures that lend themselves well to this analysis. The Utrophin gene can be divided into four regions with widely differing exon content (**Fig. 2a**). Intron 1 is 111 kb in length, and intron 50 is 101 kb long. Between these two introns, a 174-kb region contains 49 exons, whereas the 3′ 173-kb region contains the remaining 23 exons. The elongation rates within these individual regions are shown in **Table 1**; exon-rich and exon-poor gene regions seem to be transcribed at similar rates. Analysis of *ITPR1* gave a similar result (**Fig. 2d**). In this case, a 133-kb region with only five exons was compared to a 105-kb region that contains 35 exons. Again, the apparent elongation rates in these two regions were similar (**Table 1**). Also similar were the transcription elongation rates of the very long introns of two other genes, B-cell CLL/lymphoma 2 (*BCL2*) and ephrin-A5 (*EFNA5*) (**Fig. 2b**,**c** and **Table 1**).

Splicing is rapid and independent of intron length

Previous results have shown that pre-mRNA splicing can occur both co-transcriptionally and post-transcriptionally. To measure the rate of pre-mRNA splicing, we determined the time between the new synthesis of an exon and the appearance of the splicing product of that exon and the immediately preceding exon. To avoid the signal due to pre-existing mRNA in the DRB-treated cells, we used a primer in

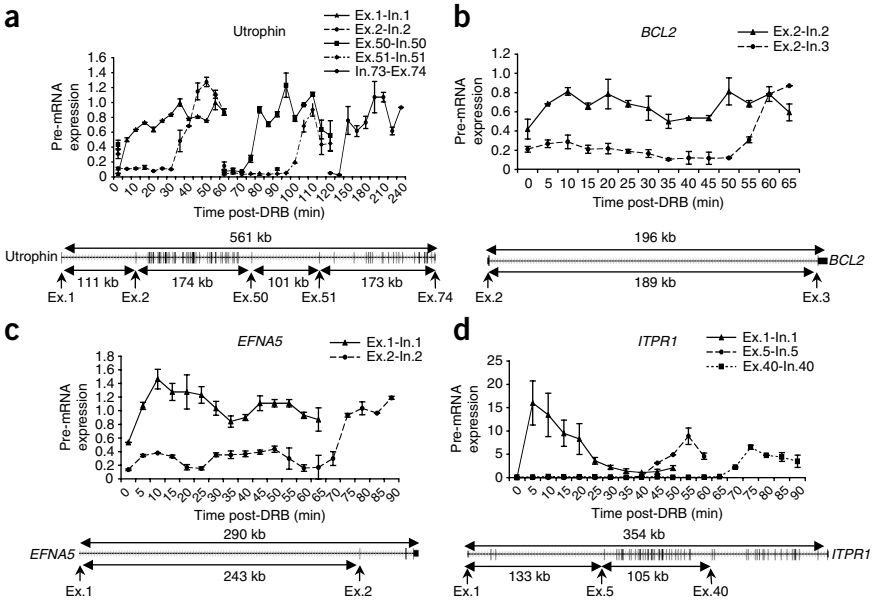

Figure 2 Kinetics of RNAPII-dependent transcription elongation. Cells were treated with DRB, and transcription was analyzed as in **Figure 1b**. (**a**–**d**) Quantitative real-time RT-PCR was performed using primer sets specific for different parts of the indicated genes to measure the levels of pre-mRNA expression. Error bars, s.e.m. The gene structure is shown below each graph, with arrows indicating the exon (Ex.)–intron (In.) junctions that were analyzed.

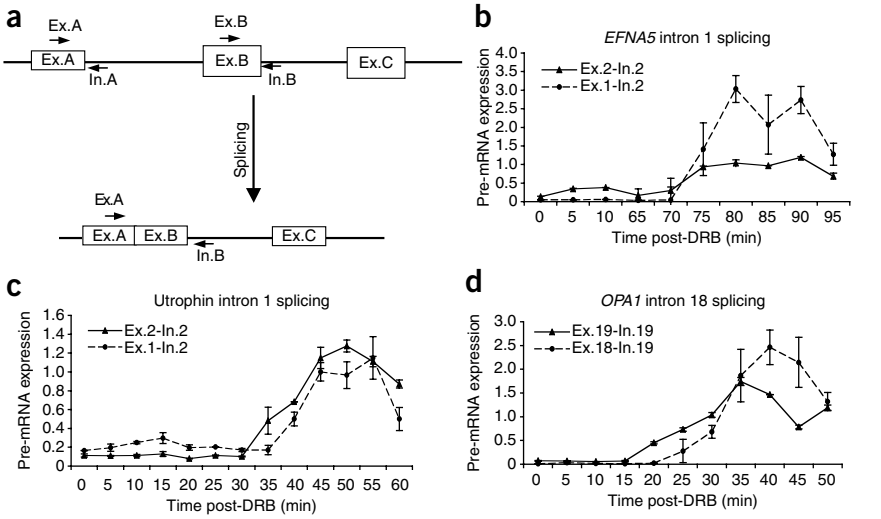

Figure 3 Kinetics of splicing of U2-dependent introns. (**a**) Schematic diagram showing the locations of primers used to measure the levels of partially spliced mRNA. Primer sets A and B detect the unspliced pre-mRNA containing the upstream and downstream exons that flank the intron, respectively. The Ex.A and In.B primer pair detects partially spliced RNA in which intron A has been spliced out but intron B remains unspliced. RNA samples from DRB-treated cells were analyzed by quantitative RT-PCR using primer pairs that detect the transcription of the exon downstream of the indicated intron or the ligated exon product of splicing. (**b**) Transcription of exon 2 (Ex.2-In.2) and splicing of intron 1 (Ex.1-In.2) of the *EFNA5* gene. (**c**) Transcription of exon 2 (Ex.2-In.2) and splicing of intron 1 (Ex.1-In.2) of the Utrophin gene. (**d**) Transcription of exon 19 (Ex.19-In.19) and splicing of intron 18 (Ex.18-In.19) of the *OPA1* gene. Error bars, s.e.m.

the downstream intron to amplify the partially spliced intermediate (**Fig. 3a**). **Figure 3b–d** shows the time course of splicing for three introns of the major or U2-dependent class. We also analyzed the splicing of six additional introns, and the results are summarized in **Table 2** (see also **Supplementary Fig. 6**).

All of these introns are spliced within 5–10 min of transcription of the downstream exon (**Fig. 3** and **Table 2**). Furthermore, this splicing must occur co-transcriptionally because the splicing reaction is completed well before the gene is transcribed to the end. For example, introns 1 and 13 of the Utrophin gene were spliced within 40 min and 60 min, respectively, after the start of transcription (**Fig. 3c** and **Supplementary Fig. 6a**), whereas the entire gene requires 140 min to transcribe (**Table 1**). We analyzed splicing of introns of widely varying sizes ranging from 1.2 kb to 243 kb (**Table 2**). Notably, there seems to be no relationship between the length of an intron and the time required to splice it. In all of the cases we analyzed, splicing of these introns occurred within 5–10 min of synthesis of the downstream exon and 3′ splice site.

U12-dependent splicing can occur co-transcriptionally

In addition to the U2-dependent introns, the human genome also contains relatively few U12-dependent introns that are spliced by a distinct spliceosome. These introns are found in genes that also contain multiple U2-dependent introns. Previous reports have shown that some U12-dependent introns are spliced more slowly than U2-dependent introns[39]. This has been suggested to be a common property of U12-dependent introns, perhaps owing to the much lower abundance of the spliceosomal small nuclear RNAs (snRNAs) that are specific to these introns or, controversially, to splicing in the cytoplasm[24].

To examine the splicing of minor class introns, we chose several large genes that contained at least one U12-dependent intron in the proximal part of the gene so that we could determine whether or not U12-dependent splicing occurs co-transcriptionally. Genes were selected that were longer than 100 kb, contained a U12-dependent intron near the 5′ end of the gene and were widely expressed.

Figure 4 shows the results of quantitative RT-PCR of these genes to detect the partially spliced transcripts resulting from splicing of each U12-dependent intron but before the splicing of the downstream U2-dependent intron. In each case, the first and last exon-intron boundaries were assayed as well as the exon immediately downstream of the U12-dependent intron and the product of U12-dependent splicing. The results were similar to those shown above for the U2-dependent introns. In each case, splicing occurred within 5–10 min of transcription of the exon downstream of the U12-dependent intron. Also, our results clearly show that U12-dependent splicing takes place before RNAPII reaches the end of the gene in every instance. Therefore, splicing of this class of introns must be nuclear.

Table 2 Time required to splice introns of different sizes and types

Gene	Intron type	Intron number	Distance from start (kb)	Intron size (kb)	Time to splice (min)	Total gene size (kb)
Utrophin	U2	1	0.15	111	5	561
Utrophin	U2	13	155	2.8	10	561
Utrophin	U2	43	245	1.5	5	561
Utrophin	U2	50	285	101	5	561
EFNA5	U2	1	0.15	243	5	294
OPA1	U2	18	52	1.2	5	104
ITPR1	U2	44	284	2.1	5	354
CTNNBL1	U2	3	43	9	5	178
CTNNBL1	U2	5	63	7.5	5	178
KiFAP3	U12	7	40	2.7	5	153
CTNNBL1	U12	4	52	11	10	178
SLC9A9	U12	7	270	4.5	10	583
IFT80	U12	2	14.8	3	10	142

DISCUSSION

The results presented here demonstrate a simple and efficient method to study the rates of transcriptional elongation and pre-mRNA splicing in endogenous human genes in their natural chromatin environment. Using this technique, we were able to measure the average rate of RNAPII transcription over genomic distances of hundreds of kilobases by examining transcription of large human genes. Our results show that, over large chromosomal distances, the average rate of RNAPII transcription is approximately 3.8 kb min^{-1}. This rate is remarkably consistent among the genes analyzed (**Table 1**) and is similar in both the cell line used here (Tet-21) and in another human cell line, HEK293 (data not shown).

We also examined our results for a relationship between gene expression level and transcriptional elongation rate. To obtain an estimate of gene expression levels, we used quantitative RT-PCR levels of pre-mRNA spanning the first exon-intron junctions of the genes listed in **Table 1**. These values are uncalibrated, but they are probably more indicative of transcriptional activity than the relative levels of mature mRNAs. Within the set of genes in **Table 1**, Utrophin and the optic atrophy 1 gene (*OPA1*) had the highest expression levels, whereas *CTNNBL1* had the lowest, with a relative difference of 15–20 fold. Inspection of **Table 1** shows that these three genes have similar apparent

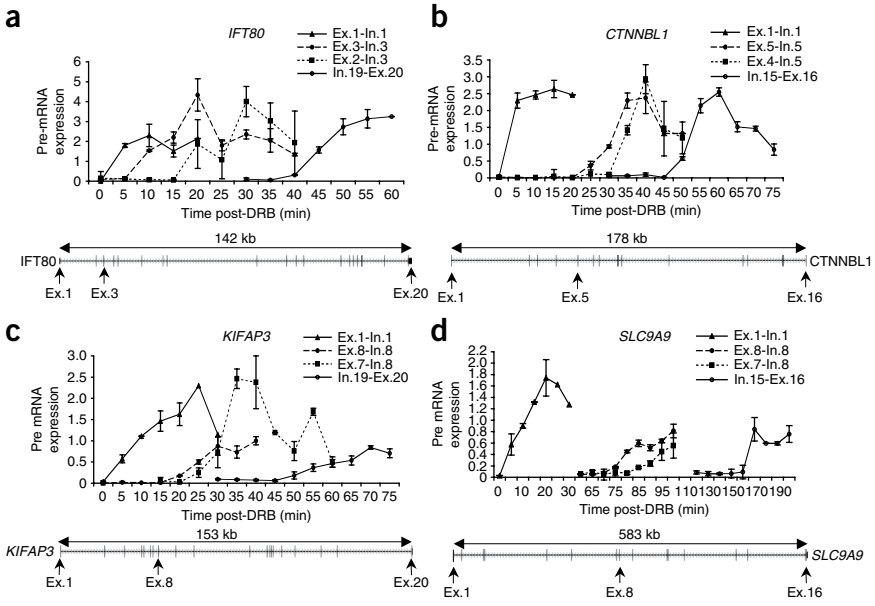

Figure 4 Kinetics of splicing of U12-dependent introns. RNA samples from DRB-treated cells were analyzed by quantitative RT-PCR using primer pairs that detect the transcription of the exon downstream of the indicated intron or the ligated exon product of splicing. (**a**) Transcription of exons 1 (Ex.1-In.1), 3 (Ex.3-In.3) and 20 (In.19-Ex.20) and splicing of intron 2 (Ex.2-In.3) of the *IFT80* gene. (**b**) Transcription of exons 1 (Ex.1-In.1), 5 (Ex.5-In.5) and 16 (In.15-Ex.16) and splicing of intron 4 (Ex.4-In.5) of the *CTNNBL1* gene. (**c**) Transcription of exons 1 (Ex.1-In.1), 8 (Ex.8-In.8) and 20 (In.19-Ex.20) and splicing of intron 7 (Ex.7-In.8) of the kinesin-associated protein 3 gene (*KIFAP3*) gene. (**d**) Transcription of exons 1 (Ex.1-In.1), 8 (Ex.8-In.8) and 16 (In.15-Ex.16) and splicing of intron 7 (Ex.7-In.8) of the solute carrier family 9 gene (*SLC9A9*). Error bars, s.e.m.

elongation rates. Thus, within the limits of our measurements, there does not seem to be a strong relationship between elongation rate and transcriptional activity.

Our measured apparent elongation rate is considerably faster than several previous estimates that fell in the range of 1.1–2.5 kb min^{-1} (refs. 14,15,18,40). Many of these studies examined single genes that were transcriptionally silent before their activation. This may put them in a different chromatin environment from that of genes that are being continuously transcribed, such as those analyzed here. Notably, our observed elongation rate is about 80% of the reported maximum rate of RNAPII transcription[17]. Darzacq *et al.* derived a maximal rate of elongation of 4.3 kb min^{-1} and a residence time for paused polymerases of about 4 min. Comparing our average rate over long genes to the maximum rate found by Darzacq *et al.* suggests that at least the leading polymerases in our long genes pause very little or only for much briefer time periods than measured by Darzacq *et al.*[17]. For example, over 100 kb, the time difference between an elongation rate of 3.8 kb min^{-1} and a rate of 4.3 kb min^{-1} would be about 3 min, which, in turn, is less than the 4-min pause time found by Darzacq *et al.*[17]. Thus, for the genes investigated here, the results suggest that RNAPII transcribes at close to its maximum rate, with few or no pausing events over hundreds of kilobases of chromatin.

We also observed that the rate of transcription was similar over long distances of pure intronic sequence or exon-rich sequences. The Utrophin gene in particular provided a means to address this point, as it contains two >100-kb introns as well as regions of >100 kb with more than 30 introns. As there is evidence for the coupling of transcription and splicing (see below), these results show that, at least for these genes, this coupling does not seem to slow down the progress of the polymerase as it transcribes multiple exons and splice sites.

We were also able to measure the rate of pre-mRNA splicing in these large genes by following the synthesis of partially spliced RNA, where the two upstream exons are spliced together but the downstream intron remains unspliced. These intermediates could be distinguished from mature mRNA because of their partially unspliced component. An unexpected finding of our study is that splicing occurred at a similar rate for several U2-dependent introns spanning a wide range of sizes. We found lag times for splicing of 5–10 min for introns ranging from 1.2 kb to 240 kb (**Table 2**). These times represent the time, after synthesis of the downstream exon, for the appearance of the spliced exons. The splicing rates for small introns agree well with previous measurements[19,20]. However, this seems to be the first report for the rate of splicing of introns greater than 100 kb in length. The speed with which long introns are spliced suggests that there are mechanisms for keeping the 5′ splice site near the elongating polymerase to allow for efficient joining to the newly synthesized 3′ splice site. Possible mechanisms include recursive splicing[41] and association of the 5′ exon with the CTD of RNAPII[21,42–46].

We also investigated the splicing of four U12-dependent introns. We found that these introns were spliced about two times more slowly than the U2-dependent introns. This result is consistent with previous data showing that these introns are spliced more slowly than comparable U2-dependent introns[39]. However, the previous study reported larger rate differences than we have observed. The 10-min splicing rates observed for U12-dependent introns suggest that their slow splicing may not represent a significant impediment to expression of their host genes, as has been suggested by previous work[39].

Another significant finding from our study is that pre-mRNA splicing occurs co-transcriptionally, irrespective of the class of introns. For U2-dependent introns, this is in close agreement with many other reports[4,21,22]. For U12-dependent introns, however, our results are in direct contradiction to a recent report that argued that the U12-dependent spliceosome machinery resides predominantly in the cytoplasm and that therefore most U12-dependent splicing must take place in the cytoplasm after the pre-mRNA is fully transcribed and transported to the cytoplasm[24]. Our results show that splicing of U12-dependent introns occurs long before the ends of the genes are transcribed. Thus, from a temporal perspective, these introns are spliced co-transcriptionally, which directly counters the hypothesis of Konig *et al.*[24] and lends unequivocal support to other reports that U12 spliceosomal complexes reside in the nucleus and function there[26,27,29].

METHODS

Methods and any associated references are available in the online version of the paper at http://www.nature.com/nsmb/.

Note: Supplementary information is available on the Nature Structural & Molecular Biology website.

ACKNOWLEDGMENTS

We wish to thank R. Dietrich and S. Saikia for technical assistance, J. Shohet (Baylor College of Medicine) and M. Schwab (Deutsches Krebsforschungszentrum)

for cell lines used in this study, D. Price for suggesting the use of DRB and D. Luse for careful reading of the manuscript. This work was supported by grants to R.A.P. from the US National Institutes of Health and the Ralph Wilson Medical Research Foundation.

AUTHOR CONTRIBUTIONS

R.A.P. conceived and coordinated the project. J.S. performed all experimental work and compiled the data. Both authors analyzed the data and wrote the manuscript.

Published online at http://www.nature.com/nsmb/.
Reprints and permissions information is available online at http://npg.nature.com/reprintsandpermissions/.

1. Rasmussen, E.B. & Lis, J.T. *In vivo* transcriptional pausing and cap formation on three *Drosophila* heat shock genes. *Proc. Natl. Acad. Sci. USA* **90**, 7923–7927 (1993).
2. Proudfoot, N.J., Furger, A. & Dye, M.J. Integrating mRNA processing with transcription. *Cell* **108**, 501–512 (2002).
3. Neugebauer, K.M. On the importance of being co-transcriptional. *J. Cell Sci.* **115**, 3865–3871 (2002).
4. Bentley, D.L. Rules of engagement: co-transcriptional recruitment of pre-mRNA processing factors. *Curr. Opin. Cell Biol.* **17**, 251–256 (2005).
5. Hirose, Y. & Manley, J.L. RNA polymerase II is an essential mRNA polyadenylation factor. *Nature* **395**, 93–96 (1998).
6. Hirose, Y., Tacke, R. & Manley, J.L. Phosphorylated RNA polymerase II stimulates pre-mRNA splicing. *Genes Dev.* **13**, 1234–1239 (1999).
7. de la Mata, M. *et al.* A slow RNA polymerase II affects alternative splicing *in vivo*. *Mol. Cell* **12**, 525–532 (2003).
8. Cáceres, J.F. & Kornblihtt, A.R. Alternative splicing: multiple control mechanisms and involvement in human disease. *Trends Genet.* **18**, 186–193 (2002).
9. Core, L.J. & Lis, J.T. Transcription regulation through promoter-proximal pausing of RNA polymerase II. *Science* **319**, 1791–1792 (2008).
10. Batsché, E., Yaniv, M. & Muchardt, C. The human SWI/SNF subunit Brm is a regulator of alternative splicing. *Nat. Struct. Mol. Biol.* **13**, 22–29 (2006).
11. Roberts, G.C., Gooding, C., Mak, H.Y., Proudfoot, N.J. & Smith, C.W. Co-transcriptional commitment to alternative splice site selection. *Nucleic Acids Res.* **26**, 5568–5572 (1998).
12. Howe, K.J., Kane, C.M. & Ares, M. Jr. Perturbation of transcription elongation influences the fidelity of internal exon inclusion in *Saccharomyces cerevisiae*. *RNA* **9**, 993–1006 (2003).
13. Kornblihtt, A.R. Chromatin, transcript elongation and alternative splicing. *Nat. Struct. Mol. Biol.* **13**, 5–7 (2006).
14. Tennyson, C.N., Klamut, H.J. & Worton, R.G. The human dystrophin gene requires 16 hours to be transcribed and is cotranscriptionally spliced. *Nat. Genet.* **9**, 184–190 (1995).
15. O'Brien, T. & Lis, J.T. Rapid changes in *Drosophila* transcription after an instantaneous heat shock. *Mol. Cell. Biol.* **13**, 3456–3463 (1993).
16. Femino, A.M., Fogarty, K., Lifshitz, L.M., Carrington, W. & Singer, R.H. Visualization of single molecules of mRNA in situ. *Methods Enzymol.* **361**, 245–304 (2003).
17. Darzacq, X. *et al.* *In vivo* dynamics of RNA polymerase II transcription. *Nat. Struct. Mol. Biol.* **14**, 796–806 (2007).
18. Boireau, S. *et al.* The transcriptional cycle of HIV-1 in real-time and live cells. *J. Cell Biol.* **179**, 291–304 (2007).
19. Kessler, O., Jiang, Y. & Chasin, L.A. Order of intron removal during splicing of endogenous adenine phosphoribosyltransferase and dihydrofolate reductase pre-mRNA. *Mol. Cell. Biol.* **13**, 6211–6222 (1993).
20. Audibert, A., Weil, D. & Dautry, F. *In vivo* kinetics of mRNA splicing and transport in mammalian cells. *Mol. Cell. Biol.* **22**, 6706–6718 (2002).
21. Das, R. *et al.* Functional coupling of RNAP II transcription to spliceosome assembly. *Genes Dev.* **20**, 1100–1109 (2006).
22. Listerman, I., Sapra, A.K. & Neugebauer, K.M. Cotranscriptional coupling of splicing factor recruitment and precursor messenger RNA splicing in mammalian cells. *Nat. Struct. Mol. Biol.* **13**, 815–822 (2006).
23. Kornblihtt, A.R., de la Mata, M., Fededa, J.P., Munoz, M.J. & Nogues, G. Multiple links between transcription and splicing. *RNA* **10**, 1489–1498 (2004).
24. König, H., Matter, N., Bader, R., Thiele, W. & Muller, F. Splicing segregation: the minor spliceosome acts outside the nucleus and controls cell proliferation. *Cell* **131**, 718–729 (2007).
25. Matera, A.G. & Ward, D.C. Nucleoplasmic organization of small nuclear ribonucleoproteins in cultured human cells. *J. Cell Biol.* **121**, 715–727 (1993).
26. Pessa, H.K. *et al.* Minor spliceosome components are predominantly localized in the nucleus. *Proc. Natl. Acad. Sci. USA* **105**, 8655–8660 (2008).
27. Friend, K., Kolev, N.G., Shu, M.D. & Steitz, J.A. Minor-class splicing occurs in the nucleus of the *Xenopus* oocyte. *RNA* **14**, 1459–1462 (2008).
28. König, H. & Muller, F. Minor splicing: nuclear dogma still in question. *Proc. Natl. Acad. Sci. USA* **105**, E37 (2008).
29. Steitz, J.A. *et al.* Where in the cell is the minor spliceosome? *Proc. Natl. Acad. Sci. USA* **105**, 8485–8486 (2008).
30. Marshall, N.F. & Price, D.H. Control of formation of two distinct classes of RNA polymerase II elongation complexes. *Mol. Cell. Biol.* **12**, 2078–2090 (1992).
31. Price, D.H. P-TEFb, a cyclin-dependent kinase controlling elongation by RNA polymerase II. *Mol. Cell. Biol.* **20**, 2629–2634 (2000).
32. Cheng, B. & Price, D.H. Properties of RNA polymerase II elongation complexes before and after the P-TEFb-mediated transition into productive elongation. *J. Biol. Chem.* **282**, 21901–21912 (2007).
33. Chodosh, L.A., Fire, A., Samuels, M. & Sharp, P.A. 5,6-Dichloro-1-β-D-ribofuranosylbenzimidazole inhibits transcription elongation by RNA polymerase II *in vitro*. *J. Biol. Chem.* **264**, 2250–2257 (1989).
34. Gomes, N.P. *et al.* Gene-specific requirement for P-TEFb activity and RNA polymerase II phosphorylation within the p53 transcriptional program. *Genes Dev.* **20**, 601–612 (2006).
35. Capranico, G. *et al.* The effects of camptothecin on RNA polymerase II transcription: roles of DNA topoisomerase I. *Biochimie* **89**, 482–489 (2007).
36. Mondal, N. & Parvin, J.D. DNA topoisomerase IIα is required for RNA polymerase II transcription on chromatin templates. *Nature* **413**, 435–438 (2001).
37. Khobta, A. *et al.* Early effects of topoisomerase I inhibition on RNA polymerase II along transcribed genes in human cells. *J. Mol. Biol.* **357**, 127–138 (2006).
38. Der, S.D., Zhou, A., Williams, B.R. & Silverman, R.H. Identification of genes differentially regulated by interferon α, β, or γ using oligonucleotide arrays. *Proc. Natl. Acad. Sci. USA* **95**, 15623–15628 (1998).
39. Patel, A.A., McCarthy, M. & Steitz, J.A. The splicing of U12-type introns can be a rate-limiting step in gene expression. *EMBO J.* **21**, 3804–3815 (2002).
40. Ucker, D.S. & Yamamoto, K.R. Early events in the stimulation of mammary tumor virus RNA synthesis by glucocorticoids. Novel assays of transcription rates. *J. Biol. Chem.* **259**, 7416–7420 (1984).
41. Burnette, J.M., Miyamoto-Sato, E., Schaub, M.A., Conklin, J. & Lopez, A.J. Subdivision of large introns in *Drosophila* by recursive splicing at nonexonic elements. *Genetics* **170**, 661–674 (2005).
42. Fong, N., Bird, G., Vigneron, M. & Bentley, D.L. A 10 residue motif at the C-terminus of the RNA Pol II CTD is required for transcription, splicing and 3′ end processing. *EMBO J.* **22**, 4274–4282 (2003).
43. Zeng, C. & Berget, S.M. Participation of the C-terminal domain of RNA polymerase II in exon definition during pre-mRNA splicing. *Mol. Cell. Biol.* **20**, 8290–8301 (2000).
44. Hirose, Y. & Ohkuma, Y. Phosphorylation of the C-terminal domain of RNA polymerase II plays central roles in the integrated events of eucaryotic gene expression. *J. Biochem.* **141**, 601–608 (2007).
45. Dye, M.J., Gromak, N. & Proudfoot, N.J. Exon tethering in transcription by RNA polymerase II. *Mol. Cell* **21**, 849–859 (2006).
46. Rosonina, E. & Blencowe, B.J. Analysis of the requirement for RNA polymerase II CTD heptapeptide repeats in pre-mRNA splicing and 3′-end cleavage. *RNA* **10**, 581–589 (2004).

ONLINE METHODS

Cell culture. We grew a derivative of the neuroblastoma cell line SH-EP Tet-21 (ref. 47), provided by J. Shohet with permission from M. Schwab, in RPMI medium (Mediatech) and 10% (v/v) FBS (Atlanta Biologicals), supplemented with 0.8% L-glutamine and 100 units ml^{-1} penicillin and 0.1 mg ml^{-1} streptomycin (Mediatech). We obtained HT1080 fibrosarcoma cells from ATCC and grew them in DMEM (Mediatech) with 10% (v/v) FBS supplemented with 0.8% L-glutamine and 100 units ml^{-1} penicillin and 0.1 mg ml^{-1} streptomycin.

Inhibition and re-initiation of transcription. We grew cells overnight on 60-mm plates to 70–80% confluency and then treated them with 100 μM DRB (Sigma) in culture medium for 3 h. We washed the cells twice with PBS to remove the DRB and then incubated them in fresh medium for various time periods. Following the incubation period, we lysed the cells directly and isolated the total RNA using a High Pure RNA isolation kit (Roche), as per the manufacturer's instructions. Actinomycin D (Sigma) or α-amanitin (Sigma), whenever used, were added at a concentration of 1 μg ml^{-1} and 2 μg ml^{-1}, respectively. CPT (Sigma) was used at 15 μM concentration and was added 15 min before completion of the DRB treatment. The PBS that was used for subsequent washings also contained 15 μM CPT, and then fresh medium containing 15 μM CPT was added to the cells for various time periods.

Induction of gene expression by interferon-β. We used HT1080 fibrosarcoma cells to study the rate of elongation of interferon-β–inducible genes. We grew cells overnight to ~80% confluency in 60-mm cell culture dishes and then treated them with 1,000 units ml^{-1} of interferon-β (Calbiochem) for 5–40 min. We harvested the cells at various time points to isolate the total RNA for quantitative RT-PCR.

Quantitative RT-PCR. We carried out reverse transcription using ImProm-II reverse transcriptase (Promega), as per the manufacturer's instructions using random hexamer primers (Promega) and 1 μg RNA per 20 μl reaction. We used the cDNA (1 μl per well) for quantitative RT-PCR, which we carried out using the iQ-SYBR Green Supermix and an iQ-iCycler (Bio-Rad). We designed the real-time primers spanning the exon-intron junctions of various genes using the IDT primer-designing software PrimerQuest on the Integrated DNA Technologies (IDT) website (http://www.idtdna.com). All primers were purchased from IDT and the sequence information for all of the primers used is available in **Supplementary Table 1**. We checked all the primers for their specificity, first *in silico* (http://genome.ucsc.edu) and then by standard PCR, before using them for quantitative PCR. A total of 40–50 PCR cycles were performed in a two-step cycling procedure with an initial denaturation step at 94 °C for 3 min and subsequent steps of 94 °C for 15 s and 60 °C for 30 s. The calculated threshold values were determined by the maximum curvature approach and ΔCt was calculated as $Ct^{GAPDH} - Ct^{sample}$. Final values for each sample were plotted relative to the value in control cells, which was set to 1.0. Reactions were performed in triplicate. Results are shown as means with s.d. from a single experiment.

Chromatin immunoprecipitation. We grew cells on 150-mm plates to 80% confluency and treated them with DRB for 3 h. We then washed them, added fresh medium and then harvested the cells at various time points. Subsequently, we fixed the cells with 1% (v/v) formaldehyde and we performed ChIP assays using a ChIP-IT Express Kit (Active Motif) as per the manufacturer's instructions. We carried out immunoprecipitations using antibodies specific to RNAPII (N20, Santa Cruz Biotechnology) and with an isotype-matched IgG control. We reserved one-tenth of each chromatin sample as the total input DNA. We then de–cross-linked the immunoprecipitated chromatin fragments and used them as templates for either real-time or standard PCR reactions using primers complementary to various exon-intron junctions of various genes. We carried out standard PCR using the Hot-start-IT PCR enzyme (USB) in a three-step cycling procedure with an initial denaturation at 94 °C for 2 min and subsequent steps of 35–40 PCR cycles at 94 °C for 30 s, 60 °C for 30 s and 72 °C for 1 min.

Gene structure and splice site identification. We obtained all of the sequence information used for designing the exon-intron junction primers for the genes used in this study from the University of California at Santa Cruz (UCSC) genome browser (http://genome.ucsc.edu). We performed the splice site determination (U2-dependent versus U12-dependent) using SpliceRack (http://katahdin.cshl.edu/SpliceRack).

47. West, A.B. *et al.* N-myc regulates parkin expression. *J. Biol. Chem.* **279**, 28896–28902 (2004).

doi:10.1038/nsmb.1666